

Spheroidal expansion and freeze-out geometry of heavy-ion collisions in the few-GeV energy regime

J. KOŁAŚ^{(1)(*)}, W. FLORKOWSKI⁽²⁾, T. GALATYUK⁽³⁾⁽⁴⁾, M. GUMBERIDZE⁽⁴⁾,
S. HARABASZ⁽³⁾, M. KURACH⁽¹⁾, R. RYBLEWSKI⁽⁵⁾, P. SALABURA⁽²⁾,
J. STROTH⁽⁴⁾⁽⁶⁾ and H. ZBROSZCZYK⁽¹⁾

⁽¹⁾ *Warsaw University of Technology - Warsaw, Poland*

⁽²⁾ *Jagiellonian University - Cracow, Poland*

⁽³⁾ *Technische Universität Darmstadt - Darmstadt, Germany*

⁽⁴⁾ *GSI, Helmholtzzentrum für Schwerionenforschung GmbH - Darmstadt, Germany*

⁽⁵⁾ *IFJ-PAN, Institute of Nuclear Physics Polish Academy of Sciences - Cracow, Poland*

⁽⁶⁾ *Institut für Kernphysik, Goethe-Universität - Frankfurt, Germany*

received 23 July 2024

Summary. — The dissatisfactory results provided by various transport models to HADES Au+Au collisions have prompted a novel approach to the description of particle spectra. The use of statistical-hadronisation-based models is proposed. In addition, a unique freeze-out hypersurface parametrisation is employed, which, with few kinematic parameters, is able to describe spectra of most abundant particles produced in the Au+Au $\sqrt{s_{NN}} = 2.4$ GeV most central collisions. A femtoscopic correlation study of identical pions is showcased with moderate reproduction.

1. – Introduction

In recent years, the low-energy regime of heavy-ion collisions (HIC) has shown discrepancies between the real-world data and models describing it [1]. The HADES Collaboration found in the transverse mass distribution of π mesons that no transport model tested in the provided reference could correctly describe their results. This notion has pushed them to look into alternative theoretical approaches to the model description of their data.

1.1. Area of study. – In order to quantify the validity of our approach, we have decided to focus on the problem in question. The chosen dataset is HADES Au+Au most central collisions (0-10%). Our perspective was to test a thermal-based model at few-GeV, in the centre of mass, energy area of HIC. A HIC event generator that utilises any theoretical model must fulfil certain assumptions upon which the theory was built. In our case it

(*) E-mail: jedrzej.kolas.dokt@pw.edu.pl

was, upon other, the thermalisation. Due to the lack of a clear theoretical understanding in this region of the phase diagram, it is highly debatable whether a thermalised medium is present at the low-energy range [2-5].

1.2. THERMal heavy-IoN GenerATOR. – The chosen thermal-based model is the THERMINATOR 2 [6], which utilises a single freeze-out approach of the constant temperature freeze-out hypersurface. It was found applicable at the ultra-relativistic energies of HIC but was not tested at the lower energies at which the HADES operates. The aim of our study was to quantify the applicability of the THERMINATOR 2 model for few-GeV HIC. The simplicity of this model has made it the best candidate for a qualitative verification of our goal.

1.3. Resonance decay. – The transverse mass spectra depend on primordial particles but also the decay product of short-lived resonances. At the few-GeV energy regime, the main contribution to the final spectra stems from the fireball itself. However, the $\Delta(1232)$ resonance showcases a non-negligible contribution to the pion spectra at the HADES energies. This notion has prompted a study of the resonances. In the original version of THERMINATOR 2, the resonance decay is performed using a fixed value of the Γ factor and mass. We are in the process of implementing a more realistic approach using mass-dependent variable width Breit-Wigner distribution [7] for all short-lived resonances and the Pok-Man-Lo [8] distribution in the case of $\Delta(1232)$.

1.4. Femtosopic correlation. – The correlation between pairs of particles emitted during the HIC, with nearly equal momenta, resembles a sensitivity to the space-time structure of the HIC. The method of study of this principle is known as the femtosopic correlation method, which can be described using the Koonin-Pratt Equation [9, 10].

The femtosopic correlation is sensitive to the shape of the source function: a time-independent function of the emission hypersurface. Any modification done to the source function should result in a different correlation function. A desired effect which we would like to utilise during our study.

2. – Spheroidal Siemens-Rasmussen model

The THERMINATOR model allows for a user-defined freeze-out hypersurface and expansion profile. Our parametrisation is based on the Siemens-Rasmussen model. The starting point is the Cooper-Frye formula [11]:

$$(1) \quad E_p \frac{dN}{d^3p} = \int d^3\Sigma_\mu(x) p^\mu f(p, x)$$

where:

$$\begin{aligned} f(p, x) &= \text{phase-space distribution function of particles} \\ p^\mu &= \text{four momentum vector } (p^\mu = (E_p, \vec{p})) \\ E_p &= \text{mass-shell energy } (E_p = \sqrt{m^2 + \vec{p}^2}) \end{aligned}$$

We settled on a spheroid shape along the beam axis with a non-constant transverse flow profile. The most critical aspects of our model are the parametrisations of position:

$$(2) \quad x^\mu = (t, r\sqrt{1-\epsilon} \cos \phi \sin \theta, r\sqrt{1-\epsilon} \sin \phi \sin \theta, r\sqrt{1+\epsilon} \cos \theta)$$

and flow:

$$(3) \quad u^\mu = \gamma(\xi)(t, \nu(\xi)\sqrt{1-\delta} \cos \phi \sin \theta, \nu(\xi)\sqrt{1-\delta} \sin \phi \sin \theta, \nu(\xi)\sqrt{1+\delta} \cos \theta)$$

Both four-vectors are represented in the spherical coordinates, where ϵ and δ are parameters modifying the deformation of a sphere. Here we assume: $\delta \in \mathbb{R} \cup \langle 0, 1 \rangle$ and $\epsilon \in \mathbb{R} \cup (-1, 0)$.

On top of that, we propose the following radial flow profile (similar to what is proposed in [12]):

$$(4) \quad \nu(r) = \tanh Hr$$

These equations introduce three kinematic parameters: ϵ , δ and H that are free to be established. Those parameters may vary according to collision centrality and energy. In our case, the best parameter values were found, which reproduce the HADES Au+Au $\sqrt{s_{NN}} = 2.4$ GeV most central collisions to the greatest degree. More information can be found in [13].

2.1. Thermal parameters. – THERMINATOR 2 uses the Cooper-Frye formalism to simulate heavy-ion collisions using a predefined freeze-out hypersurface and thermal production. Therefore, it requires parameters describing those quantities as input. It is possible to reproduce abundant particle species using temperature, chemical potentials, and freeze-out radius. In order to do so, one has to obtain mentioned quantities.

Knowing the complete formula of eq. 1 and particle abundances, it is possible to solve a set of Cooper-Frye Equations for thermal parameters analytically, as it has been done in [14]. Another option involves the use of Hadron Resonance Gas (HRG) models for the calculation of the thermal landscape of the fireball. Such an approach has been performed by Motornenko et al. [15] in response to results from Harabasz et al. [14]. The authors argue about the degeneracy of the parameter set describing the thermal equilibrium and the unphysical aspects of results obtained by Harabasz et al. Moreover, the authors were able to showcase comparisons of results depending on the approach to the production of the light fragments in HADES.

The analysis presented here combines the ambiguous case of the description of HADES Au+Au data using statistical hadronisation models with the two approaches to the emission of light fragments. Moreover, a comparison between the spherical and spheroidal symmetry is showcased. In search of a definitive description of the collisions, three cases were taken into consideration of the momentum observables ($m_T = \sqrt{k_T^2 + m_0^2}$ and $y = \frac{1}{2} \log \frac{E+p_z c}{E-p_z c}$): Spherical, following the reasoning of Harabasz et al. and its spheroidal modification, Case A, together with its counterpart Case B, from Motornenko et al.. Analogously, the femtoscopic study focuses on the production of light fragments: coalescence (Case A and Case B) *versus* thermal (Case C). The exact values of the thermal parameters used for all of the mentioned cases can be found in [13].

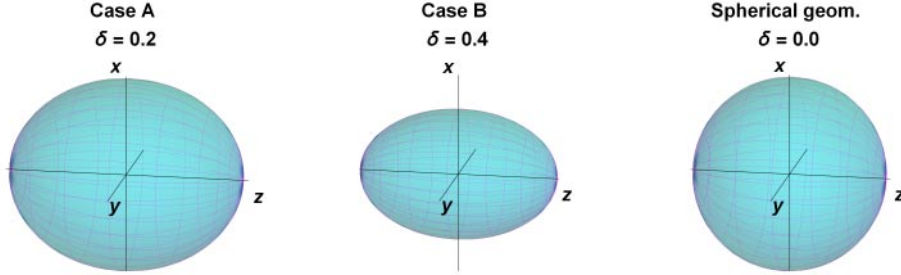


Fig. 1. – Graphical representation of the flow parametrization for the three cases studied for the kinematic observables. The points on the surfaces represent solutions of the equation $(v_x^2 + v_y^2)/(1 - \delta) + v_z^2/(1 + \delta) = v^2$. Taken from [13].

3. – Results and discussion

The results presented focus on showcasing two aspects of our study. The reasoning behind the shift towards the spheroidal symmetry of our parametrisation, and the differences between coalescence and thermal approach to the production of ${}^2\text{H}$, ${}^3\text{H}$, and ${}^4\text{He}$.

The kinematic parameters ϵ , δ and H can be divided between studied observables. The m_T and y distributions are invariant of ϵ , and coincidentally, femtoscopic correlation results are invariant of δ and H . Below are presented best-fit results of the transverse momentum and rapidity distributions, together with HBT results for different values of not yet constrained ϵ .

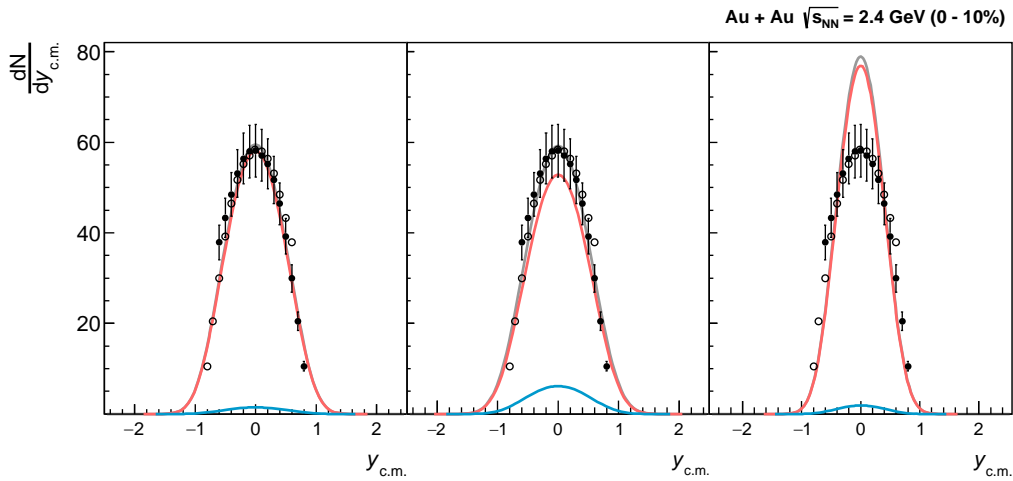


Fig. 2. – Experimental (points) and model predicted (lines) rapidity distribution of protons for three analysed cases: case A (left panel), case B (middle panel), and Spherical (right panel).

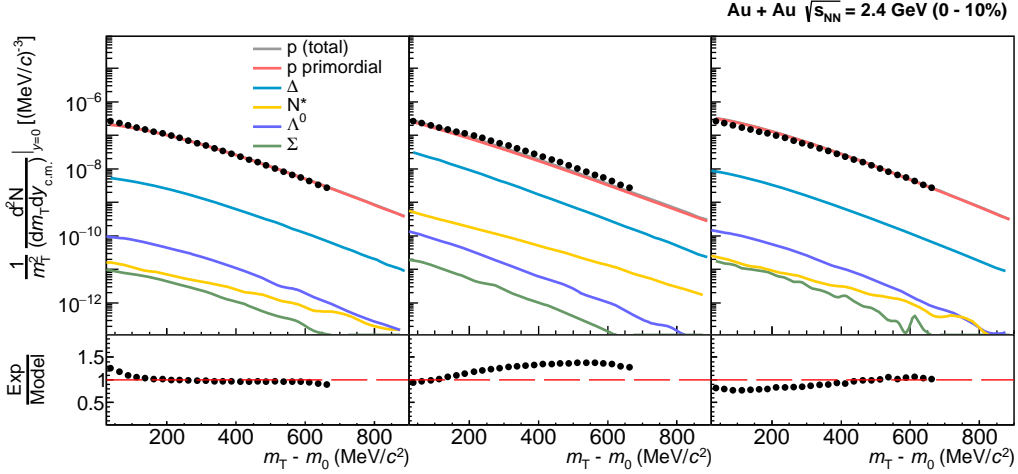


Fig. 3. – Experimental (points) and model predicted (lines) mid-rapidity transverse mass distribution of protons for three analysed cases: case A (left panel), case B (middle panel), and Spherical (right panel). The model predicts that most of the produced protons come from the fireball itself (primordial), therefore the total distribution (gray line) is shadowed by the primordial distribution (red line). Bottom plot showcases ratio between experimental points and model prediction (gray line).

3.1. Spectra distributions of abundant particles. – The introduction of the spheroidal symmetry was a necessary step, reinforced by the showcased rapidity distribution of the spherical hypersurface. Figure 2 shows a lack of longitudinal flow, which is granted by the δ parameter in our newly proposed parametrisation. The different colours stand for contributions from different proton sources.

Aside from their drastically different thermal parameters, Cases A and B resemble close similarities in the transverse mass distribution of protons (fig. 3). It is essential to note the importance of the variety of chosen observables when studying the validity of the model. The discrepancy between data and model in the Spherical case is not strongly visible.

The distribution of pions (negative), presented in fig. 4, showcases a substantial contribution from $\Delta(1232)$ resonance. In Case B, it plays a dominant role at low values of m_T . The significance of this contribution sparked the idea to look at the $\Delta(1232)$ more closely. Together with the primordial pions, it creates a double-slope, which more closely reproduces the experimental data.

3.2. Delta(1232) and other resonance treatment. – The reproduction of the invariant mass spectrum of $\Delta(1232)$ would be a great indicator of a correct implementation of the mass distribution of short-lived resonances. In order to correctly reproduce the Delta(1232) mass, other resonances also require modification. Therefore, aside from the PML distribution, the masses of all other resonances present in the THERMINATOR model were sampled from a variable-width BW distribution. This part of the work still needs to be finished and has yet to yield conclusive results. As of today, Case B is most favourable by this approach.

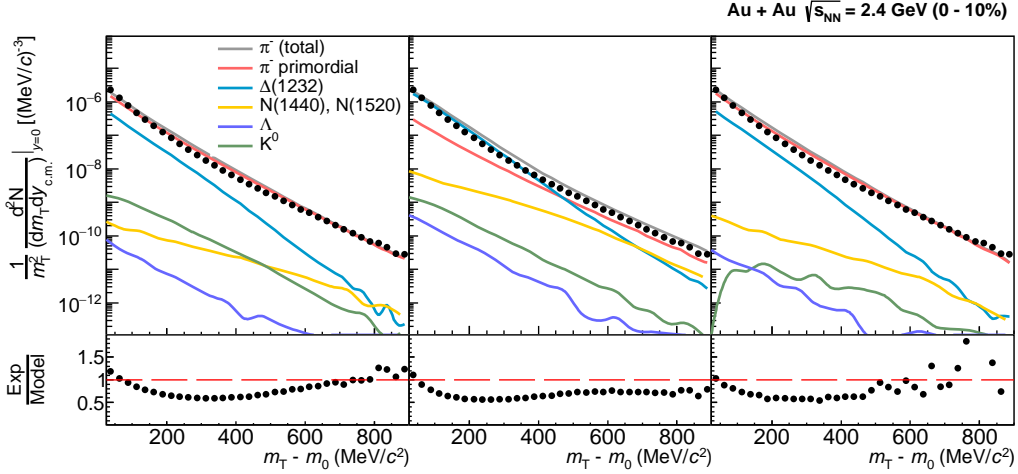


Fig. 4. – Experimental (points) and model predicted (lines) mid-rapidity transverse mass distribution of negative pions for three analysed cases: case A (left panel), case B (middle panel), and Spherical (right panel). Bottom plot showcases ratio between experimental points and model prediction (gray line).

3.3. The femtoscopy of the spheroidal model. – The results of HBT were not influenced by δ and H . It was possible to separate those two observables and study them separately. The experimental results are taken from [16, 17]. Given the satisfactory reproduction of the pion spectra, we decided to check if it is possible also to reproduce a more complex

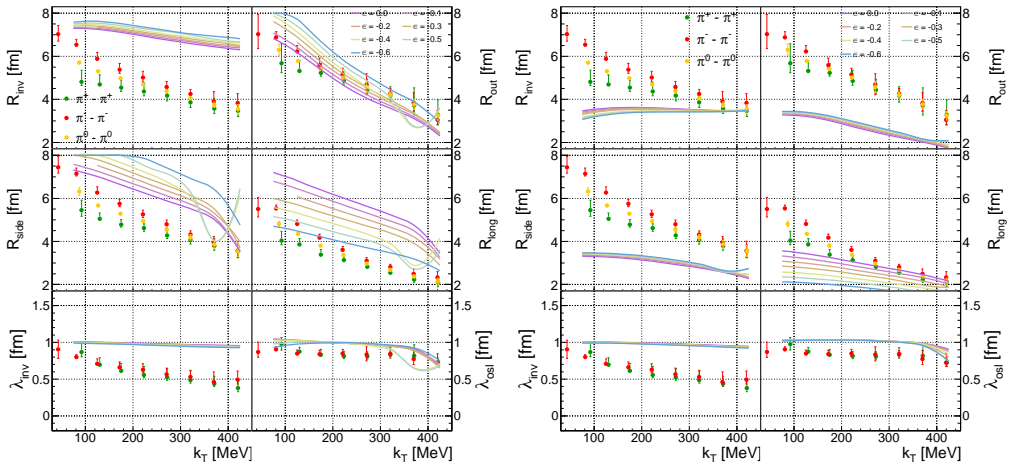


Fig. 5. – HBT Radii dependence on transverse pair momentum in the *inv*, *out*, *side*, *long* directions together with their corresponding coherence parameters λ_{inv} and λ_{osl} . Experimental results (points) are compared with the model (lines) for different values of the eccentricity-like parameter ϵ obtained for Cases A (left) and B (right).

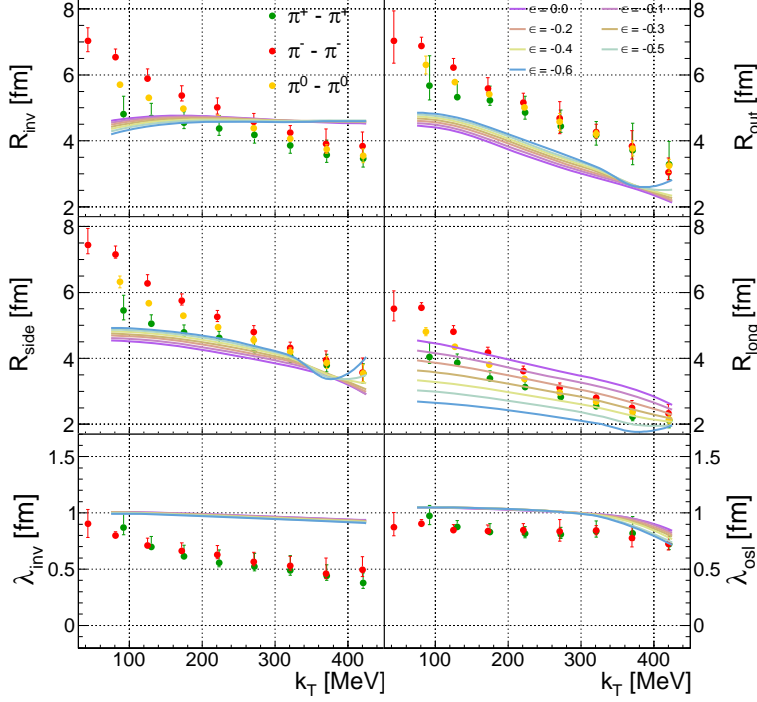


Fig. 6. – HBT Radii dependence on transverse pair momentum in the *inv*, *out*, *side*, *long* directions together with their corresponding coherence parameters λ_{inv} and λ_{osl} . Experimental results (points) are compared with the model (lines) for different values of the eccentricity-like parameter ϵ obtained for Case C.

observable, the HBT radii. The results in fig. 5 still need to be conclusive. Both cases, which involve the coalescence approach, show no resemblance with the experimental results.

Case C, showcased in fig. 6, is fairly well reproduced based on the available data. The calculated invariant radius shows a reasonably close match with the experimental results. It does not follow the observed k_T scaling and is mostly independent of the eccentricity-like parameter ϵ . Out of all the directions, long demonstrates potential applicability of further study or any constraint on the ϵ parameter.

* * *

This work was supported in part by: the Polish National Science Center Grants No. 2018/30/E/ST2/00432, No. 2017/26/M/ST2/00600, No. 2020/38/E/ST2/00019, No. 2021/41/B/ST2/02409 and No. 2022/47/B/ST2/01372; IDUB-POB-FWEiTE-3, project granted by Warsaw University of Technology under the program Excellence Initiative: Research University (ID-UB); TU Darmstadt, Darmstadt (Germany): HFHF, ELEMENTS:500/10.006, GSI F&E, DAAD PPP Polen 2018/57393092; Goethe-University, Frankfurt(Germany): HFHF, ELEMENTS:500/10.006. The author acknowledges the scholarship grant from the GET INVolved Programme of FAIR/GSI.

REFERENCES

- [1] HADES COLLABORATION, *Eur. Phys. J. A*, **50** (2020) 1.
- [2] STAUDENMAIER J., WEIL J., STEINBERG V., ENDRES S. and PETERSEN H., *Phys. Rev. C*, **98** (2018) 5.
- [3] GALATYUK T., HOHLER P. M., RAPP R., SECK F. and STROTH J., *Eur. Phys. J. A*, **52** (2016) 5.
- [4] LANG A., BLÄTTEL B., KOCH V., WEBER K., CASSING W. and MOSEL U., *Phys. Lett. B*, **245** (1990) 2.
- [5] ENDRES S., VAN HEES H., WEIL J. and BLEICHER M., *Phys. Rev. C*, **92** (2015) 1.
- [6] CHOJNACKI M., KISIEL A., FLORKOWSKI W. and BRONIOWSKI W., *Comput. Phys. Commun.*, **183** (2012) 3.
- [7] FROELICH I., BOADO L. C., GALATYUK T., HEJNY V., HOLZMANN R., KAGARLIS M., KÜHN W., MESSCHENDORP J. G., METAG V., PLEIER M. A. *et al.*, *Pluto: A Monte Carlo simulation tool for hadronic physics*, in *11th International Workshop on Advanced Computing and Analysis Techniques in Physics Research (ACAT 2007)*, 2007.
- [8] LO P. M., FRIMAN B., MARCZENKO M., REDLICH K. and SASAKI C., *Phys. Rev. C*, **96** (2017) 1.
- [9] KOONIN S. E., *Phys. Lett. B*, **70** (1977) 1.
- [10] PRATT S. and TSANG M. B., *Phys. Rev. C*, **36** (1987) 6.
- [11] COOPER F. and FRYE G., *Phys. Rev. D*, **10** (1974) 1.
- [12] SCHNEDERMANN E., SOLLFRANK J. and HEINZ U., *Phys. Rev. C*, **48** (1993) 5.
- [13] HARABASZ S., KOLAŚ J., RYBLEWSKI R., FLORKOWSKI W., GALATYUK T., GUMBERIDZE M., SALABURA P., STROTH J. and ZBROSZCZYK H., *Phys. Rev. C*, **107** (2023) 3.
- [14] HARABASZ S., FLORKOWSKI W., GALATYUK T., GUMBERIDZE M., RYBLEWSKI R., SALABURA P. and STROTH J., *Phys. Rev. C*, **102** (2020) 5.
- [15] MOTORZENKO A., STEINHEIMER J., VOVCHENKO V., STOCK R., and STOECKER H., *Phys. Lett. B*, **822** (2021) 136703.
- [16] HADES COLLABORATION, *Eur. Phys. J. A*, **56** (2020) 5.
- [17] HADES COLLABORATION, *Phys. Lett. B*, **795** (2019) 446.